2D and 3D visualization of ductile fracture

Arnaud Weck[(a)]*, David S. Wilkinson[(a)], Hiroyuki Toda[(b)] and Eric Maire[(c)]

[(a)] Department of Materials Science and Engineering, McMaster University

1280 Main Street West, Hamilton, ON L8S 4L7, Canada.

[(b)] Department of Production Systems Engineering, Toyohashi University of Technology, Toyohashi 441-8580, Japan

[(c)] G.E.M.P.P.M, INSA de Lyon, 20, avenue Albert Einstein, 69621 Villeurbanne cedex, UMR CNRS 5510, France.

*Corresponding author, E-mail: weckag@mcmaster.ca, Phone: +1 (905) 525-9140, Fax: +1 (905) 528-9295

The final stage of the ductile fracture process that leads to the failure of the material, i.e. the coalescence of the voids, occurs over small strain increments. This makes it hard to observe, and explains the lack of experimental results in the literature. The present contribution focuses on in-situ tensile testing of two new model materials, specially created to capture the coalescence event. The first is tested in a scanning electron microscope (SEM) and enables us to observe the coalescence in 2D. The second model material is tested in an X-Ray computed tomography set-up and provides 3D views of the ductile fracture process.

The use of model materials to simplify the observation of a given phenomena is not new. From the use of bubble rafts to simulate the bonding and packing of atoms and observe the behavior of dislocations in solids[1] to the use of laser-induced defects on the surface of materials for fatigue studies[2], model materials have proven to be extremely useful in helping to understand fundamental phenomenon. In the field of ductile fracture, several

model materials have been proposed – for example, Babout et al. (2000) [3], Gammage et al. (2004) [4], Magnusen et al. (1988) [5], Jia et al. (2002) [6] and Nagaki et al. (1997) [7]. However, they provide limited information on the last stage of the ductile fracture process that leads to fracture. For this we have focused on developing new model materials that allow us to capture the coalescence event and ultimately improve the predictions of ductile fracture models. As shown in Fig.1 the first material consists of a single sheet containing 10microns in diameter holes all the way through the sheet (2D approach) and for the second material, the sheet is bonded on both sides by hole-free sheets (3D approach). Different arrays of holes can be drilled to study the effect of the void configuration on the ductile fracture process. In this paper, we report on square hole arrays with lines of holes aligned at 15° and 45° to the tensile axis.

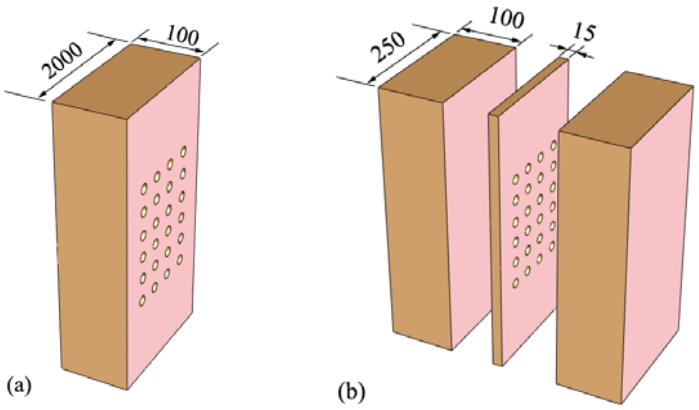

Figure1.: Drawing of the 2D model material (a) and exploded drawing of the 3D model material (b). Dimensions are in microns.

Results and Discussion: To capture the coalescence event, one needs to be able to follow the deformation of the sample as it is deforming. This is the reason for choosing the two experimental methods presented here: in-situ tensile testing in a scanning electron microscope and in an X-Ray computed tomography set-up.

The first model material represents a 2D approach and can then be observed from the surface only in a SEM. Fig.2(a) shows a typical SEM picture of a copper sample containing a regular array of laser drilled holes. The sample is then pulled slowly in-situ at an initial speed of 30microns/sec which was reduced to 1micron/sec close to the coalescence event. The test is regularly paused during the straining process and pictures are acquired to record the deformation history of the sample. Fig.2 and Fig.3 represent such sequences of deformation for the different square arrays oriented at 15° and 45° to the tensile axis. In Fig.2c and in Fig.3c the coalescence event is just about to happen. From such a sequence, one can also extract precisely the local strains between the holes if appropriate markers are placed on the sample surface. Such a study is in progress and will be reported elsewhere.

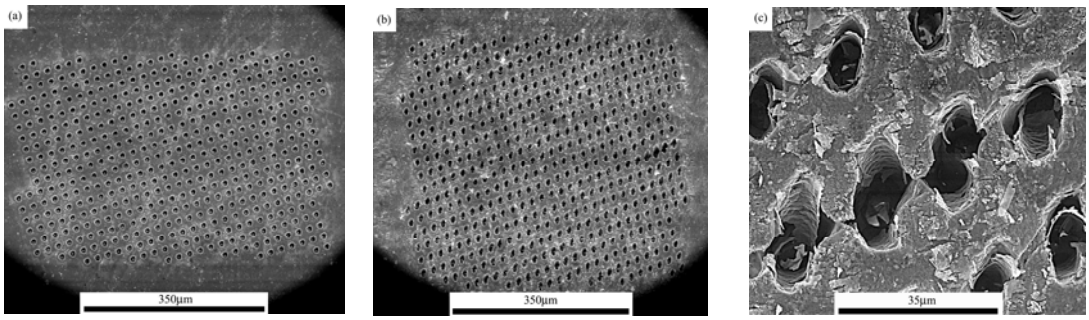

Figure 2.: Deformation sequence for a copper sample with a rectangular array of holes oriented at 15° with respect to the tensile axis. (a) undeformed sample (b) sample right at the coalescence event (c) part of the array of holes showing coalescence occurring by internal necking between the voids. Tensile direction is vertical.

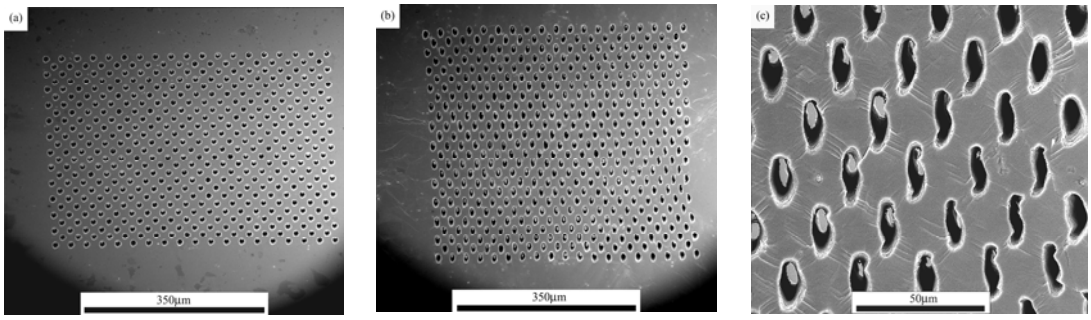

Figure 3.: Deformation sequence for a copper sample with a rectangular array of holes oriented at 45° with respect to the tensile axis. (a) undeformed sample (b) sample right at the coalescence event (c) part of the array of holes showing strong shearing between the voids and its effect on the shape of the holes. Tensile direction is vertical.

The X-Ray Computed Tomography experiments have been carried out at the Japanese synchrotron facility SPring-8. The in-situ tensile testing rig was built and provided by Prof. Toda's group from Toyohashi University of Technology in Japan. The high resolution (0.474microns) X-Ray experimental set-up is described elsewhere[8]. To follow the hole deformation and coalescence in real time, radiographic pictures are recorded continuously while the sample is tested in tension. The test is regularly stopped to acquire the 3D tomographic data. As for the SEM experiments described above, a sequence of deformation is then obtained. In order to see the holes, some transparency has been numerically applied to the copper matrix in Fig.4.

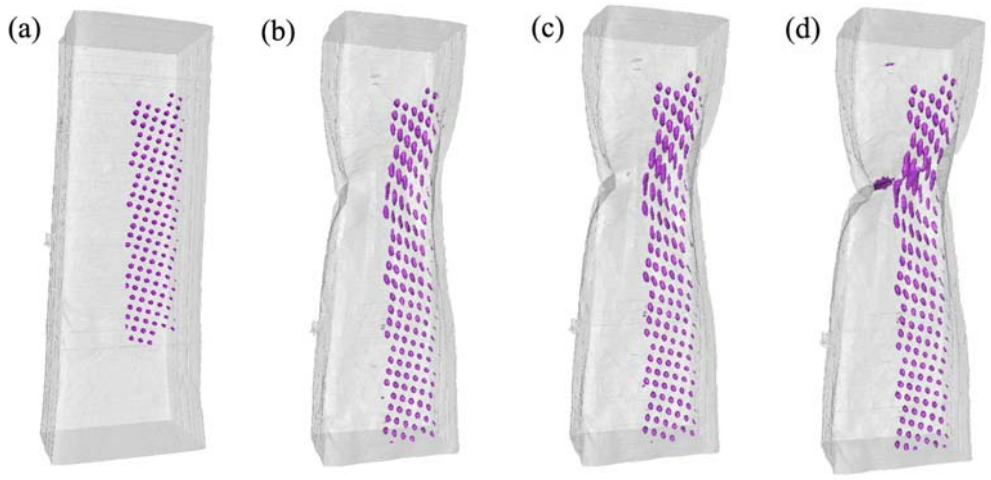

Figure 4.: Deformation sequence for a copper sample with a rectangular array of holes in 3D oriented at 15° with respect to the tensile axis. Pictures are taken at the following true strains (a) 0.00, (b) 0.40, (b) 1.16, (d) 1.42. The holes diameter is 10microns and the sample width 250microns.

A close up view on the holes shows that the coalescence event is well captured in Fig.5.

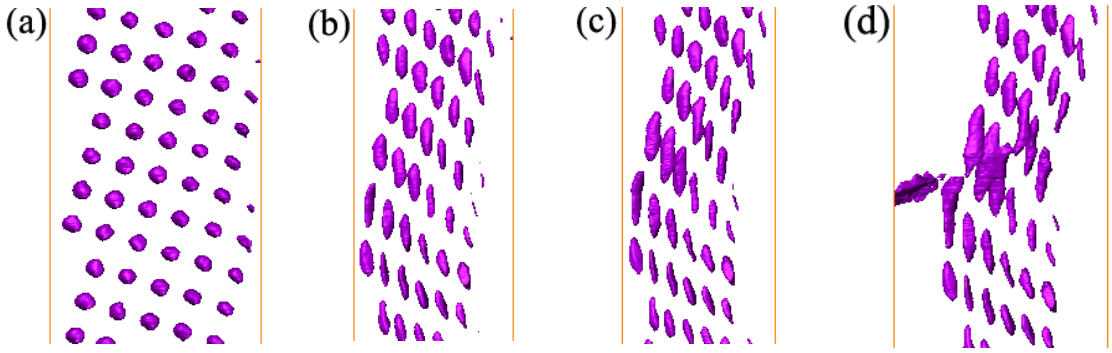

Figure 5.: Close up view of the holes deformation in the sample from Fig.4 showing the coalescence event.

From the tomography data, one can also extract the minimal cross sectional area in the sample and hence plot the true stress strain curve after necking and up to failure. Finally, the damage evolution can be calculated by taking the area fraction of voids in the smallest cross section of the sample. Fig.6 presents the plot of true stress versus true strain along with the work hardening rate and the damage for the copper sample for a rectangular array of voids oriented at 15º with respect to the tensile axis.

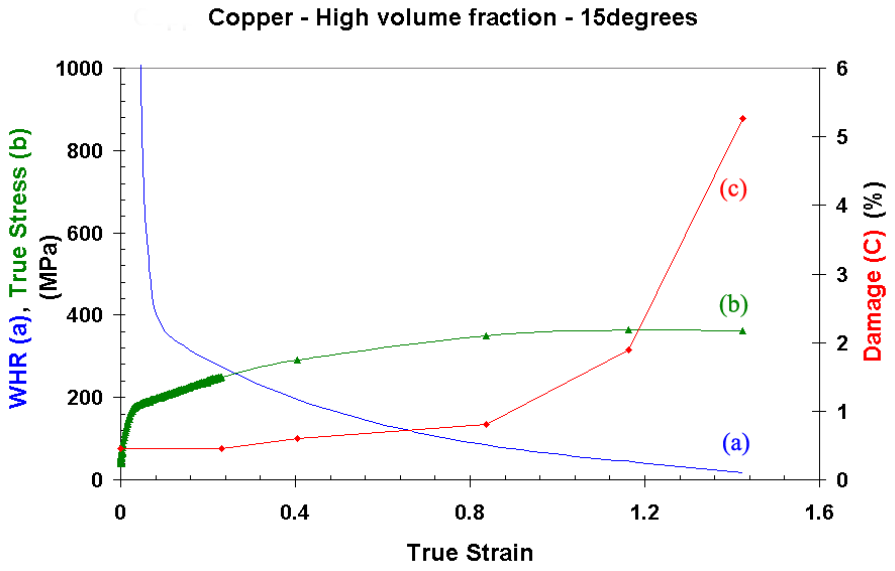

Figure 6.: True stress strain curve along with work hardening rate and damage (sample with hole array at 15º with respect to the tensile axis).

The knife-edge appearance of the material between the holes (in the fracture surface of Fig.7) tells us that the coalescence occurred by internal necking down to a point.

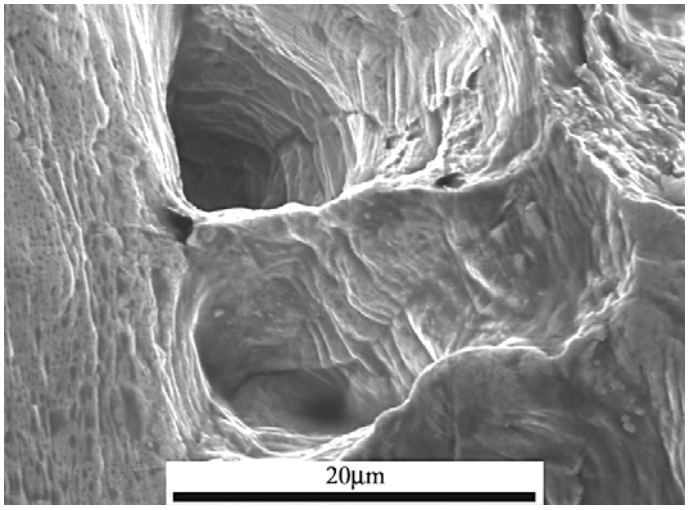

Figure 7.: SEM picture of the fracture surface of the 3D sample with hole array at 15º with respect to the tensile axis. One can see that the voids necked down to a point (without nucleation and growth of secondary void).

We have seen so far that two model materials containing regular arrays of laser drilled holes have been tested in-situ in a SEM and in an X-Ray Computed Tomography set-up. In both cases, the deformation of the holes could be followed in a controlled way, allowing the precise capture of the coalescence event between the voids (Fig.2c, Fig.3c and Fig.5). From such a deformation sequence, it is possible to extract a number of parameters as a function of the applied strain including the local strains between the voids, the void growth rate, the damage evolution, the strain rate sensitivity, the void volume fraction, etc. But of greatest interest is that all these values can be extracted exactly at the coalescence event. Such information is essential for understanding the mechanisms controlling the coalescence event and for subsequent modeling efforts. A quantitative analysis of these parameters will not be detailed here. However, some qualitative conclusions can be reached.

The results from the 2D experiments in the SEM clearly show that there are different modes of coalescence depending on the orientation of the array of holes with respect to the tensile axis. When the array is at 15° (Fig.2), the coalescence occurs by internal necking between the voids(Fig.2(c)). When the array is at 45° (Fig.3), the coalescence occurs in a shear like manner between the holes at 45°. This shearing is responsible for the shape change of the voids as shown in Fig.3(c).

When comparing Fig.2c and Fig.3c with Fig.5c, it can be seen that the void elongation at the coalescence event is much higher in the 3D case (where the final length of the voids in the tensile direction is more than 4 times the initial length of the void), than in the 2D case (where the void length is only multiplied by 2 to 3). This observation can be explained by the constraint in the 3D case due to the effect of the bonded sheets on either side of the sheet containing the array of holes. This constraining effect in 3D retards the localization between the voids, allowing more void growth. It should be noticed as well that the void volume fraction is much higher in the 2D case compared to the 3D case. This could affect the different void elongations observed between the 2D and 3D cases. The knife-edge appearance of the fracture surface (Fig.7) tells us that no population of secondary voids nucleated during fracture. The high purity of the copper samples explains this behaviour. The void growth observed in our experiments is much higher than that found in commercial purity materials, where the nucleation of secondary voids in the ligament leads to void-sheeting and decreases the failure strain as shown by Faleskog and Shih (1997) [9].

The hole arrays in 2D dictate the failure strain and the failure path in the sample. In the 3D case, the localization is delayed to higher strains and even though coalescence is observed between the holes it is now the macroscopic neck that controls the failure path in the material and not the array of holes. If a less ductile sample where to be used or a sample more sensitive to localization, one might expect to have the internal coalescence

between the voids occurring before significant amount of macroscopic necking. In that case, the array of holes might be the controlling factor in the ductile fracture process.
It would be interesting to test materials more sensitive to strain localization or with different hardening rate in order to study the effect of the strain rate sensitivity and the work hardening rate on the coalescence event. Secondary void nucleation between coalescing voids is also a phenomenon that needs more investigation considering its effect on ductility.

Conclusions: Successful 2D and 3D observations of the ductile fracture process by void growth and coalescence have been obtained on pure copper samples by in-situ tensile tests in a SEM and in a high resolution X-Ray computed tomography set-up. The coalescence event has been precisely captured and it is shown that the elongation of the voids in the 3D case is much higher that in the 2D case due to constraint effects. In the 2D case, the orientation of the array of holes with respect to the tensile axis has an effect on the failure path and on the modes of coalescence (internal necking versus shear-like failure). In the 3D case however, with the coalescence being delayed to higher strains, it is the macroscopic neck that controls the failure of the material.

Experimental

The fabrication of the new model materials used in this study is the subject of another paper and will not be detailed here. However, a simple outline is presented to provide the reader with the basic knowledge of the process. The fabrication of the first material (used for the 2D approach) consists of 2 main steps: the rolling of metallic sheets to the required thickness (100microns) and the drilling of laser holes all the way through the sheets. To fabricate the second model material (used for the 3D approach), an additional step is required whereby the sheets containing the laser drilled holes are stacked between hole-free sheets and diffusion bonded to form the 3D structure. A schematic representation of the two model materials is shown in

Fig.1. The material chosen is high purity copper (99.999%) because it has a good ductility, is able to be diffusion bonded and because of its relatively low X-Ray attenuation coefficient (important for the X-Ray computed tomography experiments). The laser holes are drilled using a femtosecond laser that allows the drilling of 10micron diameter holes all the way through 100microns thick sheets with a small heat affected zone[10-12]. The 2D model material has a cross section of 2mmX0.1mm and the 3D model material has a cross section of 0.25mmx0.215mm, necessary because of X-Ray attenuation limitations. Both materials are machined in the shape of dog bone specimens.

References

[1] K.J. Van Vliet, S. Tsikata, S. Suresh, *Appl. Phys. Lett.* **2003**, 83, 1441.
[2] R. R. Cervay, G. J. Petrak, *Engineering Fracture Mechanics* **1972,** 4, 991.
[3] L. Babout, E. Maire, J.Y. Buffière and R. Fougères, *Acta Materialia* **2001**, 49, 2055.
[4] J. Gammage, D. Wilkinson, Y. Brechet, D. Embury, *Acta Materialia* **2004**, 52, 5255.
[5] P. E. Magnusen, E. M. Dubensky, D. A. Koss, *Acta Metallurgica* **1988**, 36, 1503.
[6] S. Jia, G.F. Raiser, G.L. Povirk, *International Journal of Solids and Structures* **2002**, 39, 2517.
[7] S. Nagaki, Y. Nakayama, T. Abe, *International Journal of Mechanical Sciences* **1998**, 40, 215.
[8] K. Uesugi, Y. Suzuki, N. Yagi, A. Tsuchiyama, T. Nakano, *Nuclear Instruments and Methods in Physics Research Section A: Accelerators, Spectrometers, Detectors and Associated Equipment* **2001**, 467-468, 853.
[9] J. Faleskog, C. F. Shih, *Journal of the Mechanics and Physics of Solids* **1997**, 45, 21.
[10] A. Luft, U. Franz, A. Emsermann, J. Kaspar, *Appl. Phys. A* **1996**, 63, 93.
[11] R. Le Harzic, N. Huot, E. Audouard, C. Jonin, P. Laporte, S. Valette, A. Fraczkiewicz, R. Fortunier, *Appl. Phys. Lett.* **2002**, 80, 3886.
[12] S. Valette, E. Audouard, R. Le Harzic, N. Huot, P. Laporte and R. Fortunier, *Applied Surface Science* **2005**, 239, 381.